 doi:10.20944/preprints202208.0103.v1

Article

Oxidized Resveratrol Metabolites as Potent Antioxidants and Xanthine Oxidase Inhibitors

Orinamhe G. Agbadua[1], Norbert Kúsz [1], Róbert Berkecz [2], Tamás Gáti [3], Gábor Tóth [4] and Attila Hunyadi [1,5,*]

[1] Institute of Pharmacognosy, University of Szeged, 6720, Szeged, Hungary; orinamhe.agbadua@uniben.edu (O.G.A.); kusznorbert@gmail.com (N.K.)
[2] Institute of Pharmaceutical Analysis, University of Szeged, H-6720 Szeged, Hungary; berkecz.robert@szte.hu
[3] Servier Research Institute of Medicinal Chemistry (SRIMC), H-1031 Budapest, Hungary; tamas.gati@hu.netgrs.com
[4] NMR Group, Department of Inorganic and Analytical Chemistry, Budapest University of Technology and Economics, H-1111 Budapest, Hungary; drtothgabor@t-online.hu
[5] Interdisciplinary Centre of Natural Products, University of Szeged, H-6720 Szeged, Hungary
* Correspondence: hunyadi.attila@szte.hu; Tel.: +3662545557

Abstract: Resveratrol is a well-known natural polyphenol with a plethora of pharmacological activities. As a potent antioxidant, resveratrol is highly oxidizable, and readily reacts with reactive oxygen species (ROS). Such a reaction not only leads to a decrease in ROS levels in a biological environment but may also generate a wide range of metabolites with altered bioactivities. Inspired by this notion, in the current study, our aim was to take a diversity-oriented chemical approach to study the chemical space of oxidized resveratrol metabolites. Chemical oxidation of resveratrol and a bioactivity-guided isolation strategy using xanthine oxidase (XO) and radical scavenging activities led to the isolation of a diverse group of compounds, including a chlorine-substituted compound (**2**), two iodine-substituted compounds (**3** and **4**), two viniferins (**5** and **6**), an ethoxy-substituted compound (**7**) two ethoxy-substituted dimers (**8** and **9**). Compounds **4**, **7**, **8** and **9** are reported here for the first time. All compounds without ethoxy-substitution exerted stronger XO inhibition than their parent compound, resveratrol. By enzyme kinetic and *in silico* docking studies compounds **2**, **3** and **4** were identified as potent competitive inhibitors of the enzyme while the viniferins acted as mixed-type inhibitors. Further, compounds **2** and **9** had better DPPH scavenging activity and oxygen radical absorbing capacity than resveratrol. Our results suggest that the antioxidant activity of resveratrol is modulated by the effect of a cascade of chemically stable oxidized metabolites, several of which have significantly altered target specificity as compared to their parent compound.

Keywords: Resveratrol; antioxidant metabolism; scavengome; biomimetic oxidation; bioactivity-guided isolation; NMR spectroscopy; xanthine oxidase

1. Introduction

Resveratrol (*E*-3,5,4′-trihydroxystilbene; molecular formula: $C_{14}H_{12}O_3$) is found naturally in many common foods including a variety of berries, tomato skin, peanuts, pistachios and cocoa [1]. It is probably the most popular dietary polyphenol, with a myriad of reported pharmacological activities including anticancer, antioxidant, anti-inflammatory, cardio-protective and neuroprotective effects [2,3]. The complex pharmacology of resveratrol involves its ability to interact with many important enzymes and receptor signaling pathways, and its ability to prevent damage connected to oxidative stress. Resveratrol is known to scavenge a variety of free radicals [4], i.e., reactive oxygen and nitrogen species (ROS and RNS, respectively, collectively referred to as RONS). Such reactive species are normal byproducts of the aerobic metabolism, and, in physiological conditions, their levels are under tight enzymatic control. The imbalance between the production and detoxification of RONS may, however, lead to the production of toxic free radicals that are at

 doi:10.20944/preprints202208.0103.v1

the hallmark of a variety of pathological conditions [5]. Xanthine oxidase (XO), a molybdenum-containing metalloenzyme, is an enzyme that serves as an important biological source of ROS. XO catalyzes the oxidation of hypoxanthine to xanthine and finally, to uric acid in the presence of molecular oxygen that acts as electron acceptor, producing superoxide anion radical ($O_2^{\bullet-}$) and hydrogen peroxide (H_2O_2) [6]. High XO activity plays a major role in the onset of oxidative stress; therefore, this enzyme is a relevant target for not only gout treatment, but also to the prevention and/or perhaps treatment of a wide range of pathological conditions [7]. Resveratrol has been reported to inhibit the XO enzyme by decreasing uric acid formation and superoxide radical production [8,9].

Despite its high oral absorption rate (at least 70%) and much valued bioactivities, resveratrol has very poor systemic bioavailability (~ 0.5%) due to extensive phase I and II biotransformation in the enterocytes and liver, and to a minor extent by gut microbiota [10]. These transformations have made it difficult to identify the metabolites responsible for the observed bioactivities and thus, resveratrol metabolism and the bioactivity of the resulting metabolites has attracted great interest in recent years [11]. While there have been numerous reports on the bioactivities of glucuronidated and sulfated conjugates of resveratrol [12], limited knowledge is available on the metabolites formed via peroxidation and oxidation. Considering the free radical scavenging properties of resveratrol, however, the biological relevance of such oxidized metabolites may have been underestimated. It is an intriguing notion that the structure and function of polyphenolic antioxidants change upon RONS scavenging, and, depending on the antioxidant's chemical properties and type of ROS/RNS scavenged, a complex mixture of chemically stable oxidized metabolites may be formed from such an interaction. In some cases, such metabolites may have a dramatically altered bioactivity pattern when compared to the parent antioxidant [11]. Concerning resveratrol, a study by Shingai *et al*. reported that biomimetic, Fe-catalyzed oxidation led to a mixture containing a variety of minor products, and, despite the rather low conversion, this mixture showed potent lipoxygenase (LOX) inhibitory activity in contrast with the inactive resveratrol itself. Several active metabolites were also obtained that, however, did not fully explain the very high increase in bioactivity [13].

These are well in line with the 'scavengome' concept that considers any small molecule antioxidants as pro-drugs oxidizable by ROS/RNS to a broad chemical space of bioactive metabolites in a biological environment under oxidative stress [11,14]. To expand related knowledge on resveratrol, in the current study it was our objective to use a chemical oxidation-driven, diversity-oriented synthetic strategy to obtain its new bioactive derivatives. To simultaneously aim at obtaining biologically relevant resveratrol metabolites and their semi-synthetic analogs, we decided to involve both biomimetic and non-biomimetic approaches. To explore the biomedical potential of these oxidized resveratrol metabolites/analogues, XO was selected as the first target of our interest.

2. Materials and Methods

2.1 General information

Resveratrol **(1)** with a purity of >98% was purchased from Career Henan Chemical Co. (Henan province, China). HPLC solvents were purchased from ChemLab (Zedelgem, Belgium), organic solvents and reagents: (bis(trifluoroacetoxy)iodo)benze (PIFA), (diacetoxyiodo)benzene (PIDA), 2,2'-Azobis(2-amidinopropane) dihydrochloride (AAPH), oxone, anhydrous, monobasic, potassium phosphate (P5379), and xanthine (0626) were purchased from Sigma Aldrich (Budapest, Hungary). Periodic acid, iron (III) chloride hexahydrate and sodium periodate were purchased from Reanal Laboratory Chemicals (Budapest, Hungary).

2.2 General procedures for resveratrol oxidation

 doi:10.20944/preprints202208.0103.v1

Several oxidative reactions were carried out on resveratrol as shown in Table 1. The reactions were monitored by thin layer chromatography, solid phase: Silica 60 F254 (250 µm, Merck Co., Darmstadt, Germany); liquid phase: chloroform – ethyl acetate – formic acid (2.5:1:0.1, v/v/v) at regular intervals with visualizations performed under UV light λ_1 = 254 nm and λ_2 = 365 nm. At the end of each reaction, the mixtures were evaporated, extracted with ethyl acetate, and evaporated in vacuo. As a pre-purification step, each residue was filtrated through silica with hexane – acetone (1:1, v/v). A 10µL aliquot of each mixture was dissolved in CH_3CN and analyzed by HPLC (PU-2080 pumps; AS-2055 Plus autosampler; MD-2010 Plus PDA detector, Jasco Co., Tokyo, Japan) under the following conditions: column, Kinetex XB-C18 (250 x 4.6mm, 5_μ); solvent system, water (solvent A) and CH_3CN (solvent B): elution, linear gradient from 25% solvent B to 75% solvent B for 25 min, and then isocratic mode for 75% solvent B for 2 min; flow rate, 1mlmin^{-1}; detection, 199nm – 650nm. The purity of the isolated metabolites was also determined using same analytical HPLC condition.

Isolation and purification of metabolites from mixtures was done using an Armen Spot Prep II integrated HPLC purification system (Gilson, Middleton, WI, USA) using a Kinetex XB-C18 or Biphenyl column (250 x 21.2 mm, 5µm), and appropriately chosen eluents.

2.3 Reaction with PIFA in acetonitrile (Ox 1)

Resveratrol (300 mg) was dissolved in acetonitrile (150 ml), an acetonitrile solution of PIFA (565.14 mg / 150 ml) was added, and the mixture stirred for 5 h at room temperature. The solvent was evaporated using a rotary evaporator, and the residue was partitioned between water (150 ml) and ethyl acetate (3x 100 ml). Dry residue of the combined organic layers was purified by silica gel column chromatography eluted with acetone/hexane (1:1, v/v) and thereafter evaporated in vacuo. The residue was subsequently purified by preparative HLPC using an isocratic elution of CH_3CN-H_2O (28:72, v/v) on a biphenyl column to get compound **6** (39.80mg). **6** was further purified by HPLC on a Luna Silica column (250 x 4.6 mm, 5µm, 100Å) using an elution of cyclohexane-isopropanol (86:14, v/v) to obtain 10.13 mg of the pure compound.

2.4 Reaction of resveratrol with AAPH and $NaIO_4$ (Ox 2)

To a solution of resveratrol (500 mg) in acetonitrile (250 ml), an aqueous solution of AAPH (890 mg / 250 ml) and an acetonitrile solution of $NaIO_4$ (468.75 mg / 250 ml) were added, and the mixture was stirred for 23 h at 65°C. The reaction was stopped by adding an aqueous solution of reduced glutathione (541.12 mg / 100 ml), keeping it in the same conditions for 5 more min as before. Then it was cooled down in an ice-bath. The solvent was evaporated on a rotary evaporator, and the residue was partitioned between water (250 ml) and ethyl acetate (4x 200 ml) and evaporated to give a combined dry residue (753.96 mg). The residue was purified by preparative HLPC on a C18 column with isocratic elution of CH_3OH-H_2O (50:50, v/v) to give a fraction containing **3** (46.57 mg) and **5** (24.00 mg). The purified fractions were further separated using CH_3OH-H_2O (45:55, v/v) on same column to get compounds **3** (12.93 mg) and **5** (11.38 mg).

2.5 Reaction of resveratrol with PIDA in acetonitrile (Ox 3)

Resveratrol (100 mg) was dissolved in acetonitrile (25 ml), an acetonitrile solution of PIDA (282.20 mg / 75 ml) was added, and the mixture stirred for 2 h at room temperature. The reaction was stopped by adding an aqueous solution of reduced glutathione (269.25 mg / 30 ml). The solvent was evaporated on a rotary evaporator, and the residue was partitioned between water (100 ml) and ethyl acetate (3x100 ml). Dry residue of the combined organic layers was purified by preparative HLPC using the biphenyl column and solvent, CH_3OH-H_2O (52:48, v/v) resulting in compound ***5*** (6.37 mg).

2.6 Reaction with PIFA in ethanol (Ox 4)

To a solution of resveratrol (250 mg) in ethanol (50 ml), an ethanol solution of PIFA (471 mg / 200 ml) was added, and the mixture stirred for 90 min at room temperature. The

 doi:10.20944/preprints202208.0103.v1

reaction was stopped with an aqueous solution of reduced glutathione (673.75 mg/ 187.5 ml). The solvent was evaporated on a rotary evaporator, and the residue was partitioned between water (250 ml) and ethyl acetate (3x300 ml). Dry residue of the combined organic layers was purified by preparative HLPC on a biphenyl column with an isocratic elution of CH_3CN-H_2O (31:69, v/v) to give compounds **7** (24.80 mg), **8** (13.30 mg) and **9** (33.98 mg) (13.30 mg). Further purification was carried out on the compounds on the same column but using an elution of CH_3OH-H_2O (52:48, v/v) to obtain compounds **7** (11.93 mg) and **9** (22.62 mg). **8** was further purified by HPLC on a Luna Silica column (250 x 4.6 mm, 5µm, 100Å) using an elution of cyclohexane-isopropanol (85:15, v/v) to obtain 8.38 mg of pure compound.

2.7 Reaction of resveratrol with $FeCl_3$ and Oxone in ethanol (Ox 5)

Resveratrol (600 mg) was dissolved in ethanol (300 ml), an ethanol solution of oxone (4.05 mg / 150 ml) was added, and the mixture stirred for 5 min at room temperature. An ethanol solution of periodic acid (396 mg / 180 ml) was subsequently added, and the mixture stirred for further 7 h under same condition. The reaction was stopped by adding an aqueous solution of reduced glutathione (1615.50 mg / 150 ml). The solvent was evaporated on a rotary evaporator, and the residue was partitioned between water (250 ml) and ethyl acetate (3 x 200 ml). Dry residue of the combined organic layers was purified by preparative HLPC using a biphenyl column with an isocratic elution using CH_3OH-H_2O (54:46, v/v) to get compounds **3** (167.30 mg), **4** (61.94 mg) and a mixture containing **7** (60.21 mg). Further purification was carried out on the fractions under the same conditions as above to obtain **3** (167.30 mg), **4** (18.30 mg) and **7** (18.66 mg) in pure form.

2.8 Reaction of resveratrol with $FeCl_3$ and H_5IO_6 in acetonitrile (Ox 6)

Resveratrol (480 mg) was dissolved in acetonitrile (240 ml), an acetonitrile solution of iron chloride hexahydrate (17.04 mg / 80 ml) was added, and the mixture was stirred for 5 min at room temperature. An acetonitrile solution of periodic acid (384 mg / 450 ml) was subsequently added, and the mixture was stirred for further 17 h. The reaction was stopped by adding an aqueous solution of reduced glutathione (1293 mg / 240 ml). The solvent was evaporated on a rotary evaporator, and the residue was partitioned between water (250 ml) and ethyl acetate (3x300 ml). Dry residue of the combined organic layers was purified by preparative HLPC using a biphenyl column and an isocratic elution of CH_3OH-H_2O (51:49, v/v) to obtain compounds **2** (29.94 mg), **3** (27.06 mg) and **4** (63.61 mg). Further purification was carried out on the C18 column with isocratic elution CH_3OH-H_2O (42:58, v/v) to obtain compounds **2** (12.01 mg), **3** (9.13 mg) and **4** (22.27 mg).

2.9 Reaction of resveratrol with $FeCl_3$ and H_5IO_6 in ethanol (Ox 7)

Resveratrol (360 mg) was dissolved in ethanol (180 ml), an ethanol solution of iron chloride hexahydrate (12.78 mg / 60 ml) was added, and the mixture was stirred for 5 min at room temperature. An ethanol solution of periodic acid (396 mg / 180 ml) was subsequently added, and the mixture was stirred for further 17 h. The reaction was stopped by adding an aqueous solution of reduced glutathione (969.9 mg / 180 ml). The solvent was evaporated on a rotary evaporator, and the residue was partitioned between water (250 ml) and ethyl acetate (2x 250 ml). Dry residue of the combined organic layers was purified by preparative HLPC using a biphenyl column and an isocratic elution of CH_3OH-H_2O (51:49, v/v) to obtain a fraction mixture containing compounds **3** (107.99 mg). This fraction was further purified by preparative HPLC using a C18 with an isocratic elution of CH_3OH-H_2O (42:58, v/v) and a semi-preparative HPLC Gemini-NX C18 column (250 x 10.0 mm, 5µm) with CH_3OH-H_2O (42:58, v/v) as the eluent to get **3** (3.11 mg) in pure form.

2.10 Structure elucidation

Structure elucidation of the isolated compounds was based on their molecular formulas obtained by high-resolution mass spectrometry (HRMS) and on detailed nuclear magnetic resonance (NMR) studies. HRMS spectra were acquired on an FTHRMS-Orbitrap (Thermo-Finnigan) mass spectrometer equipped with an ESI ion source typically

 doi:10.20944/preprints202208.0103.v1

used in positive ionization mode, except for compound **2** for which both positive- and negative-mode spectra were taken (see Supplementary Material, Fig. S8-S15). ^{1}H NMR, ^{13}C, APT, HSQC, HMBC, ^{1}H,^{1}H-COSY, NOESY, one-dimensional selective NOE spectra were recorded in acetone-d_6 and DMSO-d_6 on a Bruker Avance III 500 NMR equipped with a cryo-probehead and on Bruker Avance spectrometers. Chemical shifts (δ) are given on the δ-scale and referenced to the solvents (acetone-d_6: δH = 2.05 and δC = 29.9 ppm; DMSO-d_6: δH = 2.50 and δC = 39.5 ppm); coupling constant (*J*) values are expressed in Hz. The pulse programs were taken from the Bruker software library (TopSpin 3.5). Full ^{1}H and ^{13}C signal assignment was performed by means of comprehensive one- and two-dimensional NMR methods using widely accepted strategies [15,16].

^{1}H assignments were accomplished using general knowledge of chemical shift dispersion with the aid of the ^{1}H–^{1}H coupling pattern. To facilitate the understanding of NMR signal assignments in the supplementary material the stereo structures with the δ^{1}H and δ^{13}C and *J* values are also depicted on the NMR spectra (Fig. S16–S56).

2.11 Bioactivity studies

2.11.1 Xanthine oxidase inhibitory activity

XO inhibitory activity was tested based on a modified protocol described previously by Noro *et al.* with slight modifications [17]. Briefly, reagents were 50mM phosphate buffer pH 7.5, 0.15mM xanthine solution dissolved in the phosphate buffer (pH 7.5) and 0.1U/mL XO enzyme solution. Compound solutions were prepared by dissolving in DMSO and subsequently buffer. In a 96-well UV plate, 100 µL xanthine solution was added to 150 µL solution of compounds, before adding the enzyme solution (50 µL) by pump to initiate the formation of uric acid. The increase in uric acid was determined at 290 nm for approximately 150 seconds at 37^{O}C, with allopurinol as the reference using a FluoStar Optima plate reader (BMG Labtech, Ortenberg, Germany). The XO activity of a blank and allopurinol used as a negative and positive control, respectively was also determined. The slope (m) for the compounds, blank and positive control was obtained, and the XO inhibitory activity was expressed as the percentage inhibition of XO in the above-mentioned assay mixture system, calculated as follows:

$$\% \text{ Inhibition} = 100 - (m_{compounds} / m_{blank} \times 100)$$

Dose-effect studies on the most bioactive compounds (1.5625 – 200 µM) and resveratrol (25 – 400 µM) were used to determine the concentration that inhibits 50% of the XO enzyme activity. Enzyme kinetic studies of the bioactive compounds was also performed. The sigmoidal dose–response model, dose-response inhibition curve models and Lineweaver Burk transform plots were obtained by using software GraphPad Prism 8.0 (La Jolla, CA, USA), and these were used to determine the IC_{50} values of the compounds and to determine their mode of inhibition.

2.11.2 DPPH radical scavenging activity

The DPPH free radical scavenging assay was performed based on the method of Fukumoto *et al.* [18] with some modification. One hundred microliters of 0.1mM solution of DPPH reagent prepared in methanol was added to 100µL solution of compounds at concentrations ranging from 2µM – 500µM). Absorbance of each well including the blank (containing 100 µL methanol) and standard (ascorbic acid) was measured at 550 nm for 30 minutes using a FluoStar Optima plate reader (BMG Labtech, Ortenberg, Germany). A sigmoidal dose–response model of the blank corrected values was used to calculate IC_{50} values of compounds using GraphPad Prism 8.0 (La Jolla, CA, USA).

2.11.3 Oxygen Radical Absorbance Capacity (ORAC) assay

 doi:10.20944/preprints202208.0103.v1

The oxygen radical absorbance capacity was determined as described by Dávalos *et al*. [19] with slight modifications. Briefly, the reaction was carried out in 75 mM sodium phosphate buffer (pH 7.4), and the final reaction mixture of each well in a 96-well polystyrene microplate with black sides and flat clear bottom was 200 µL. Each well consisted of 20 µL, 100 µM sample (compounds dissolved in DMSO), 70 nM fluorescein and lastly, 12 mM AAPH solution. A blank containing sodium phosphate buffer, fluorescein and AAPH, and a range of calibration solutions using Trolox TM (from 3.125 to 100 µM) as standard antioxidant were also used in each assay. All reaction mixtures were prepared in triplicate. The fluorescence was read with an excitation wavelength of 485 nm and an emission filter of 520 nm every 90 second cycle time for 120 cycles using a FluoStar Optima plate reader (BMG Labtech, Ortenberg, Germany). The antioxidant abilities, expressed as Trolox equivalents, was obtained by calculating the area under the fluorescence decay curve (AUC), and interpolating the net AUC against the Trolox standard curve done using GraphPad Prism (GraphPad version 8.0 Software, La Jolla, CA, USA).

3. Results and discussion

3.1 Preparation and evaluation of oxidized resveratrol metabolites

Resveratrol was transformed by a variety of oxidative reagents. These included hypervalent iodine (III) reagents PIFA / PIDA, and AAPH that were found in our previous studies to reasonably mimic reactions that could occur via ROS scavenging by an antioxidant [20,21]. To further increase the explorable chemical complexity, periodic acid was also selected with oxone or iron (III) chloride as a co-oxidant. As a biomimetic element in the work-up procedure, most reactions were terminated by adding reduced glutathione (GSH), an abundant intracellular antioxidant [22]. The reaction mixtures (Ox1-Ox7) were then analyzed by HPLC-PDA for their chromatographic fingerprints (Supporting Information, Figures S1-S7), and subjected to XO inhibitory assay that also served as a guidance for isolation of major bioactive metabolites. Results, along with a listing of compounds isolated from each mixture, are compiled in Table 1.

Table 1. Oxidation of resveratrol, XO inhibitory activity of the oxidized mixtures, and list of compounds isolated from each. Results are expressed as mean ± SEM, n = 3, *: p <0.05 by one-way ANOVA using Dunnett's multiple comparison test to the parent compound resveratrol. Resveratrol was tested at 100 µM, and mixtures Ox1-Ox7 at 100 µM of resveratrol equivalents.

ID	Oxidants	Experimental conditions[a]	XO Inh. (%)	Compound isolated
Resveratrol	-	-	49.9 ± 6.9	-
Ox1	PIFA	CH_3CN, r.t. 5h	42.5 ± 3.3	**6**
Ox2	AAPH, $NaIO_4$	CH_3CN, 65°C, 23h[b]	37.6 ± 5.3	**3**, **5**
Ox3	PIDA	CH_3CN, r.t., 2h[b]	32.0 ± 2.1*	**5**
Ox4	PIFA	EtOH, 2h[b]	47.1 ± 1.6	**7**, **8**, **9**
Ox5	H_5IO_6, Oxone	EtOH, r.t, 7h[b]	55.8 ± 0.9	**3**, **4**
Ox6	H_5IO_6, $FeCl_3$	CH_3CN, r.t. 17h [b]	67.8 ± 1.8*	**2**, **3**, **4**
Ox7	H_5IO_6, $FeCl_3$	EtOH, r.t., 17h[b]	75.7 ± 4.9*	**3**

[a] Experimental conditions are given as solvent, temperature, time, respectively.
[b] Reactions were terminated by adding reduced glutathione

3.2 Structure elucidation of the isolated compounds

The ^{1}H NMR spectrum of our starting material **1** *E*-resveratrol (3,5,4'-trihydroxystilbene, $C_{14}H_{12}O_3$) consists of one set of three aromatic hydrogens coupled in an AX_2 system (δ 6.54d, 2H, ^4J=2 Hz and δ 6.28t, 1H, 2 Hz), another set of four aromatic hydrogens coupled in an AA'XX' system (δ 7.24dm, 2H, ^3J=8.4 Hz and δ 6.79dm, 2H, 8.4 Hz), and two

Preprints (www.preprints.org) | NOT PEER-REVIEWED | Posted: 4 August 2022 doi:10.20944/preprints202208.0103.v1

doublet signals (δ 7.03d, 1H, ^{3}J=16 Hz and δ 6.89d, 1H, 16Hz) indicating the presence of a HC = CH double bond with *E* configuration [23].

For compound **2**, HRMS revealed an elemental composition of $C_{14}H_{11}O_3Cl$ (Supporting Material, Fig. S8-S9) indicating that one hydrogen is substituted with a Cl. The ^{1}H NMR spectrum of **2** is rather similar to that of **1**, with only one characteristic change, i.e., the original AX_2 system of the 3,5-dihydroxyphenyl moiety turned into an AX system (δH-6 6.79d, 1H, ^{4}J=2 Hz and δH-4 6.48d, 1H, 2 Hz), indicating that compound **2** is 2-chloro-*E*-resveratrol. This corroborates with previous studies by Li *et al*. [24]. To achieve complete ^{1}H and ^{13}C NMR assignment, ^{1}H, ^{13}C-APT, HSQC, HMBC, COSY, and NOESY measurements were utilized (Fig. S16-S19).

The molecular formula of both compounds **3** and **4** was established as $C_{14}H_{11}O_3I$ (Fig. S10-S11). In the ^{1}H NMR spectrum of **3** (Fig. S20), the signals of 3,5-dihydroxyphenyl moiety appeared at δ6.70 as a singlet with 2H intensity corresponding to the isochronic H-2,6 atoms, revealing the iodination at C-4. It is remarkable that in the ^{13}C spectrum, the effect of an iodine substituent is accompanied by a characteristic diamagnetic shift, as shown by δC-4 signal at 73.8 ppm (Fig. S21). Compound **3** was previously reported by Lee *et al*.[25,26] as products formed from the halogenation of resveratrol.

Compound **4** had a similar aromatic substitution pattern as that of **2**, i.e, an AX system (δH-6 6.78d, 1H, ^{4}J=2 Hz and δH-4 6.48d, 1H, 2 Hz). In the 2-iodinated-*E*-resveratrol product, the δC-2 signal appeared at 79.1 ppm. The utilized NMR spectra are compiled in Fig. S24-S27.

In the case of both compounds **5** and **6**, HRMS indicated the molecular formula of $C_{28}H_{22}O_6$ (Fig. S12–S13), and their ^{1}H NMR spectra were in good correspondence with those previously reported for δ-viniferin (**5**) and ε-viniferin (**6**) [27-29]. However, the use of non-exact names in the literature may lead to misunderstandings. In our study, both 2,3-dihyro-benzofuran derivatives were racemic mixtures. Considering the relative positions of the 2,3-substituents, one should differentiate between *cis* and *trans* diastereomers. For the sake of simplicity, only the enantiomeric forms with 2R configuration are depicted in Figure 1. Compound **5**, i.e., (*E*)-(±)-2,3-*cis*-δ-viniferin is structurally (±)-(*E*)-5-(3,5-dihydroxystyryl)-3-(3,5-dihydroxyphenyl)-2-(4-hydroxyphenyl)-*cis*-dihydrobenzofuran, whereas compound **6** (*E*)-(±)-2,3-*trans*-ε-viniferin corresponds to the (±)-6-hydroxy-(*E*)-4-(4-hydroxystyryl)-3-(3,5-dihydroxyphenyl)-2-(4-hydroxyphenyl)-*trans*-dihydrobenzofuran structure. A recent study on a series of 2,3-disubstituted dihydrobenzofuran derivatives demonstrated usefulness of the *J*(H-2,H-3) coupling constant to distinguish between *cis*/*trans* isomers [30]. Considering the approximately planar structure of the five-membered ring of dihydrobenzofurans, in the *cis* isomer (compound **5**) a dihedral angle close to zero degree is consistent with a *J*(H-2,H-3)=8 Hz coupling. On the other hand, in the case of *trans* substituents, the detected *J*(H-2,H-3)=5 Hz coupling is in accordance with a ~120° dihedral angle (see compound **6**). The NMR spectra utilized for the unambiguous structure elucidation of **5** and **6** are compiled in Fig. S28-S37).

Based on the HRMS data, an elemental composition of $C_{16}H_{22}O_5$ (Fig. S14) was established for compound **7,** indicating the incorporation of two ethoxy groups into the structure of resveratrol. In the ^{1}H and ^{13}C NMR spectra of **7** (Fig. S38-S39), signals of the 3,5-dihydroxyphenyl and 4-hydroxyphenyl moieties remained well identifiable, but instead of the H–C=C–H double bond, the signals of a diethoxy substituted chiral H–C–C–H group appeared (δH = 4.14d/ δC = 85.9 and δH = 4.18d/ δC = 85.6, *J*(H,H)=6.6 Hz). Their differentiation was supported by the NOESY and HMBC measurements (Fig. S40-S41). In the uniform NMR spectra nothing indicated the presence of a diastereomeric mixture, but neither the *J*(H,H) coupling, nor the results of NOESY experiment allowed the identification of *threo* or *erithro* configuration.

The molecular formula of **8** was established as $C_{30}H_{28}O_7$ by means of HRMS ($[M+H]^+$, calculated: 501.19078, found 501.19189), suggesting an ethoxy group attached to a dimer. The ^{1}H NMR spectrum of **8** (Fig. S43) identified the presence of four groups of aromatic hydrogens, namely two sets of four aromatic hydrogens coupled in an AA'XX' system (δ

 doi:10.20944/preprints202208.0103.v1

7.24dm, 2H, ^{3}J=8.6 Hz, δ 6.79d, 2H, and δ 7.10dm, 2H, ^{3}J=8.6 Hz, δ 6.71dm, 2H), corresponding for 4-hydroxyphenyl moieties, in addition one set of three aromatic hydrogens coupled in an AX_2 system at δ 6.36d, 2H, ^{4}J=2 Hz, δ 6.27t, 1H), (3,5-dihydroxyphenyl group) and at the and an AX system (δ 6.40d, 1H, ^{4}J=2.5 Hz, δ 6.23d, 1H). Appearance of the two doublet signals (δ 6.58d, 1H, ^{3}J=16 Hz, δ 6.89d, 1H) proved the presence of a HC = CH double bond with *E* configuration. The signals at δ 3.65q, 2H, *J*=6.8 Hz, δ 1.23t, 3H are unique to ethoxy group, whereas the δH 5.36d, 1H, ^{3}J=3 Hz and δ 4.62br, 1H signals correspond to an ethoxy and 2-substituted *E*-resveratrol substituted chiral H–C–C–H group.

The partial broadening of several ^{1}H signals refer to hindered rotation. ^{1}H, ^{13}C-APT, HSQC, HMBC, ^{1}H,^{1}H-COSY and NOESY spectra were utilized for signal assigment (Fig. S43-S48). In exploring the order of connection of different structural units of compound **8** the characteristic long-range HMBC correlations, marked with black arrows (Fig. S32) were extremely effective. Considering the uniform NMR spectra nothing indicated the presence of a diastereomeric mixture for the racemic compound **8**.

To facilitate understanding of the relative configurations of the two stereogenic centers, the *S* configuration was arbitrarily set for the O–CH- center. Examining the three staggered conformers along the H-C → C-H,OEt carbon bond the ^{3}J(H,H)=3 Hz coupling suggested that the share of the *anti*-conformer in the equilibrium is negligible. Thorough evaluation of steric proximities detected in the NOESY spectrum (red double arrows in Fig. S48) identified the only conformer that is consistent with NOESY results, *i.e. S,S* configuration of the depicted enantiomer of compound **8**.

In case of compound **9**, HRMS measurements did not provide an identifiable m/z value for the molecular ion, neither in positive nor in negative mode. Nevertheless, the ^{1}H-NMR, ^{13}C-APT, HSQC, HMBC and NOESY spectra (Fig. S49-S53) taken in acetone-d_6 clearly revealed that compound **9** is also an ethoxy-substituted dimer with a structure rather similar to that of **8**. The one characteristic difference between these compounds is that **9** contains a quaternary C–OH instead of the sp^3 CH of **8**. Due to the increased steric crowding, the rotation along the H-C → C-OH carbon bond is hindered, resulting a partial broadening of several ^{1}H and ^{13}C signals (δ CH 5.24s/81.5 and δ HO-C 4.53br ppm, and even the δ C remained under the noise level). Due to the broad CH and OH signals, the NOESY measurement did not allow detection of all the sterically close hydrogen atoms, and thus the identification of the relative configuration of the two stereogenic centers was not possible. To overcome the hindered rotation, we raised the temperature to 80°C in DMSO-d_6 (Fig. S54-S56), which made sharper the signals in the ^{1}H-NMR, ^{13}C-APT and HSQC spectra. However, the CH and C-OH signals (5.16 and 4.54 ppm) remained relatively broad. The selective one-dimensional ROE experiment on these hydrogens revealed several characteristic steric proximities (Fig. S56, see red arrows), but these did not allow a definite distinction between the possible relative configurations.

The structures of compounds **1–9** are shown in Figure 1.

Preprints (www.preprints.org) | NOT PEER-REVIEWED | Posted: 4 August 2022 doi:10.20944/preprints202208.0103.v1

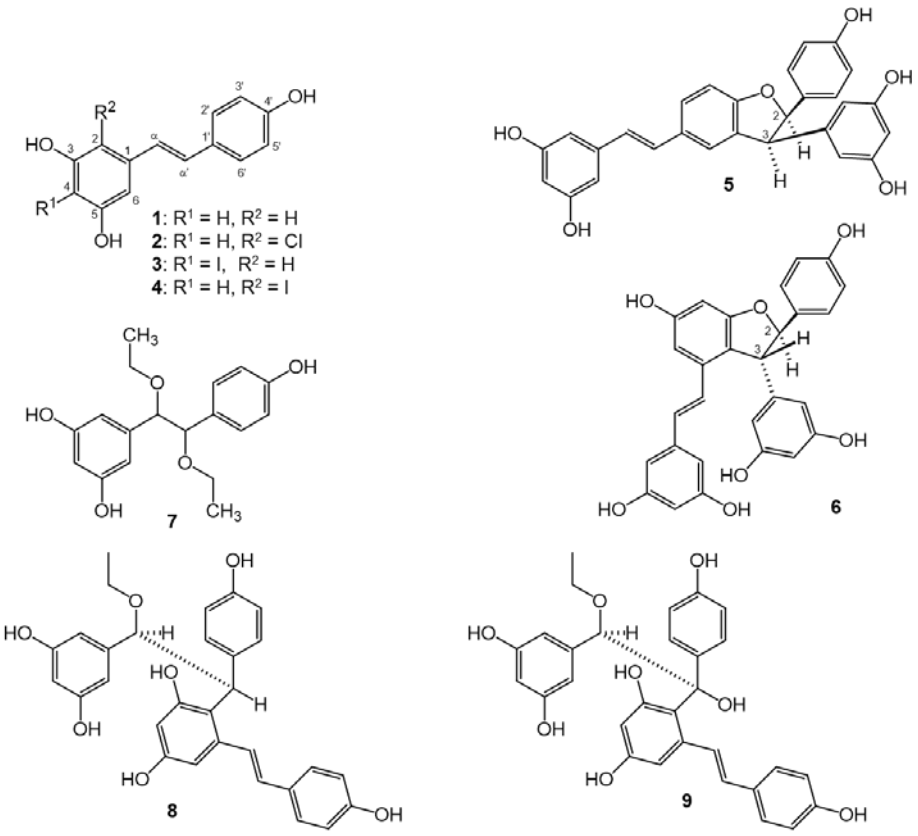

Figure 1. Structures of resveratrol (**1**) and its metabolites obtained by chemical oxidation (**2**-**9**). Each optically active compound (**5**, **6**, **8**, **9**) is racemate; for simplicity, only one enantiomer is presented. For compounds **7** and **9** the relative configuration could not be determined.

The compounds obtained represent a structural diversity that was expectable based on our chemical approach. Concerning their biological relevance, it may be worth stressing that compounds **2**, **5** and **6** are also expectable products of a resveratrol molecule scavenging free radicals in a biological environment. For example, chlorine substitution (as in compound **2**) may be the result of a reaction of a resveratrol radical with chloride ions that are abundant in intra- and extracellular liquids. Further, resveratrol molecules have strong self-association through π-π stacking in aqueous medium [31,32]. This makes radical coupling reactions, leading to dimers such as **5** and **6**, possible in a biological environment under oxidative stress regardless of the very low concentrations achievable *in vivo*. Compounds **3** and **4** are valuable to expand chemical space towards halogen substituted derivatives related to the biologically more relevant compound **2**. In addition to this, the ethoxy substituted compounds **7**-**9** are of further interest for their potential formation when resveratrol gets oxidized in the presence of ethanol, e.g., during the aging of red wine that is connected to a gradual loss of resveratrol content [33].

3.2 Bioactivity of the isolated compounds

3.2.1 Xanthine oxidase inhibitory activity

XO inhibitory activity of the compounds was estimated based on their ability to prevent uric acid formation from xanthine. Biomimetic oxidation of resveratrol resulted in the formation of some metabolites with marked increase in the ability to inhibit this enzyme with regards to resveratrol as shown in Table 2.

Table 2. XO inhibition percentage of compounds **1**-**9** at 100μM, and their IC_{50} values. Results are expressed as mean ± SEM. *: $p < 0.05$ by one-way ANOVA using Dunnett's post-hoc test as compared to resveratrol, n = 4; due to the large differences, statistical significance was not evaluated for the IC_{50} values.

Preprints (www.preprints.org) | NOT PEER-REVIEWED | Posted: 4 August 2022 doi:10.20944/preprints202208.0103.v1

Compounds	XO Inh (%)	XO IC_{50} (μM)
Resveratrol (**1**)	55.6 ±1.1	119.4 ± 2.0
2	90.6 ± 4.4	4.8 ± 0.8
3	97.2 ± 4.9*	15.3 ± 1.4
4	93.8 ± 1.3*	6.4 ± 0.5
5	77.4 ± 2.1	16.4 ± 1.3
6	69.1 ± 3.1	22.8 ± 6.3
7	14.4 ±3.0*	>1000
8	15.1 ± 1.7	233.3 ± 5.1
9	31.5 ± 4.8	234.1 ± 4.8
Allopurinol	97.3 ± 0.9*	5.9 ± 0.9

Unlike resveratrol, compounds **2,3** and **4** exerted a nearly complete inhibition of XO at 100 μM. Subsequent determination of the dose-response curves revealed that compounds **2** and **4** showed similar efficacy in XO inhibition as the reference drug allopurinol. To evaluate the mode of inhibition of the isolated active compounds, enzyme inhibition kinetics studies were performed. Our results revealed that compounds **2, 3** and **4** inhibit XO competitively, i.e., they bind to the active center of the enzyme. The viniferins (**5** and **6**) were observed to be mixed-type inhibitors, and they are reported here for the first time as potent inhibitors of XO. Lineweaver-Burk transform plots of compounds **2**-**6** are presented in the Supplementary Material, S57-S61.

Subsequently to the enzyme kinetic studies, *in silico* docking was performed with the most potent competitive inhibitors **2** and **4**. To this, we followed our previously published approach using the 3NVY protein, and the docking site was defined in a 10Å radius around the experimental position of quercetin bound to the active site of XO [34]. Results for the best-docked poses are presented in Figure 2.

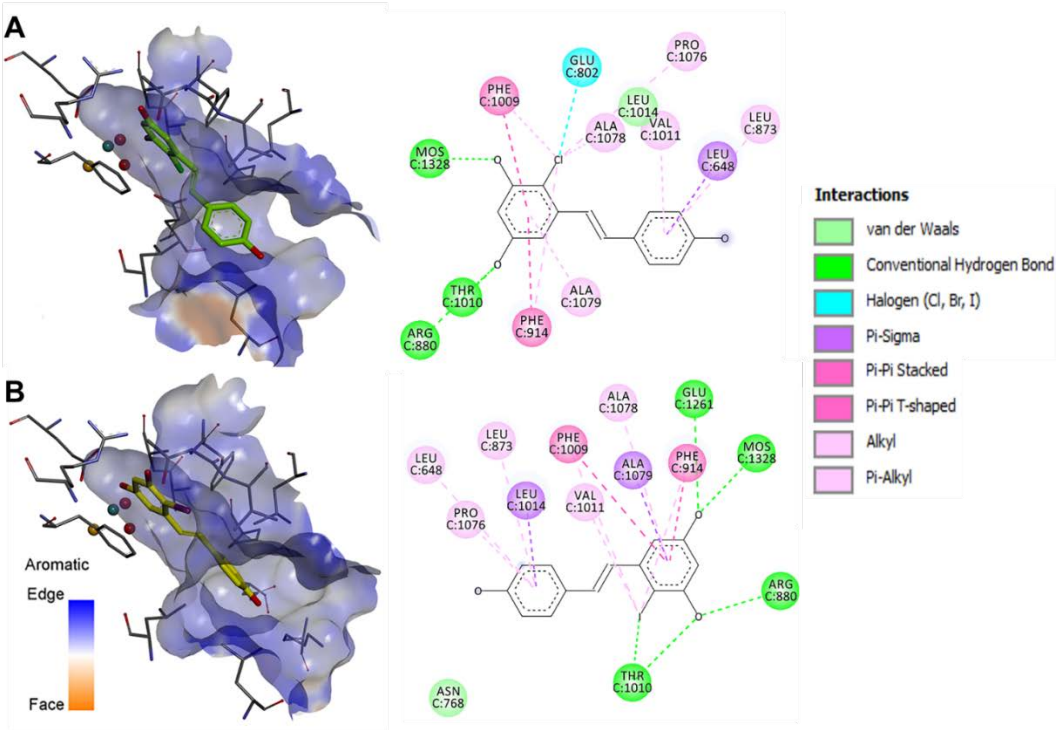

Figure 2. Best docked poses of compounds **2** (**A**) and **4** (**B**). 3D orientation and aromatic edge/face receptor surface is shown for both compounds at identical viewing angle and zoom (left), along with the 2D interpretation of the ligand-residue interactions with the 3NVY protein (right).

 doi:10.20944/preprints202208.0103.v1

In the best docked orientation of **2** and **4** in the active site, several hydrogen bonds were observed between the phenolic ring containing the two meta-hydroxy groups and several amino acid residues. In both compounds, a H-bond was observed with the molybdopterin residue, Mos1328. The halogens found in **2** and **4** formed a H-bond with Glu802 and Thr1010, respectively. The orientation of **2** and **4** in the active site of XO was further stabilized by π–π interactions between the compounds' A-ring and the aromatic ring of residues Phe914 and Phe1009. Interaction with these amino acids constrained the compounds to a well-defined plane perpendicular to the base plane of the molybdenum center in the active site.

Proton transfer from the molybdopterin residue's hydroxyl group to Glu1261 is an initial step required for the conversion of xanthine to uric acid by XO. Glu802, Arg880, Thr1010 have also been reported to be essential in the catalytic transformation of xanthine to uric acid [35,36]. Therefore, interactions observed between **2** and **4** and these residues provide a reasonable mechanistic background to the compounds' XO inhibitory activity. The orientation and interactions of the hydroxy groups of **2** and **4** are similar to the 5-OH and 7-OH of quercetin and apigenin, both of which are well-studied as XO inhibitors [34]. Planarity, extended conjugation and, in case of flavones, the presence of a 7-OH group were reported as the key features for small-molecule XO inhibitors [34,37,38]. These rules apply for several stilbenes and flavonoids, and XO inhibition is an activity that fits well to their widely acknowledged antioxidant effect *in vivo* [39].

3.2.2 *Free radical scavenging activity*

To assess the compounds' potential direct antioxidant activity in comparison with that of resveratrol, their DPPH scavenging activity and oxygen radical absorbing capacity (ORAC) was also evaluated. These two antioxidant assays are somewhat complementary to each other, since DPPH may be scavenged through either single-electron transfer (SET) or hydrogen atom transfer (HAT), while reaction mechanism in the ORAC assay is mainly HAT [40]. Results are presented in Table 2.

Table 2: ORAC values and DPPH radical scavenging activity of compounds **1**-**9**. Results are expressed as mean ± SEM. *: $p < 0.05$ by one-way ANOVA using Dunnett's multiple comparison test to the parent compound, resveratrol. n = 2 for DPPH and 3 = ORAC assay.

Compounds	DPPH IC_{50} (μM)	ORAC (Trolox Equivalents, TE)
Resveratrol (**1**)	27.7 ± 1.4	8.9 ± 0.2
2	15.8 ± 1.0	9.9 ± 0.5
3	41.0 ± 1.5	11.6 ± 0.2*
4	51.7 ± 1.6	12.5 ± 0.7*
5	340.7 ± 2.1	6.3 ± 0.3
6	92.1 ± 1.6	15.2 ± 0.5*
7	>500	8.1± 0.5
8	53.1 ± 1.5	13.9 ± 0.1*
9	22.6 ± 1.9	9.5 ± 0.3

In this study, the DPPH free radical scavenging activity of resveratrol corroborated with some earlier reports [41,42], and, expectably, it was found a potent antioxidant also in the ORAC assay as reported before [43].

Notably, several of the oxidized derivatives of resveratrol was found similarly or more potent free radical scavenger than their parent compound in either or both bioassays. Concerning structure-activity relationships, it was found that substituting one of the aromatic rings with chlorine, as in compound **2**, increased the DPPH scavenging activity, unlike iodine substitution (**3** and **4**). Iodine substitution, however, significantly increased the compounds' capacity for HAT. Substitution of a phenol ring with electron-donating

 doi:10.20944/preprints202208.0103.v1

or electron-withdrawing groups markedly alters the antioxidant activity of polyphenols [44], and substitution with electron-withdrawing halogens modulates free radical scavenging activity depending on the position and the number of halogen substituents [45]. The presence of halogens was reported to confer increased potential for HAT [46], which is in agreement with our results on the iodine-substituted compounds **3** and **4**. The ethoxy-substituted dimer **8** also had higher TE value than resveratrol, and similar antioxidant abilities were reported for other resveratrol dimers without the benzofuran ring [47].

(*E*)-(±)-2,3-*trans*-ε-viniferin (**6**) was also more potent than resveratrol concerning its ability to neutralize peroxyl and alkoxyl radicals produced by AAPH [48], which is likely a direct consequence of its higher number of phenolic hydroxyl groups prone to HAT reactions.

4. Conclusions

The chemical oxidation of resveratrol led to the formation of a chemically diverse set of new metabolites. Several of the compounds obtained are expectably among those that may be formed when resveratrol scavenges ROS/RNS in a biological environment. Three ethoxy substituted compounds were also obtained in which the solvent ethanol reacted with resveratrol's oxidized intermediates; these compounds may have relevance as possible constituents of aged red wines.

Except for the ethoxy derivatives, all compounds showed greater XO inhibitory activities than resveratrol, and the most potent chlorine substituted compound **2** by nearly two orders of magnitude. Further, when compared to resveratrol, most compounds were similarly, or more potent free scavengers of DPPH radicals and/or $ROO^{\cdot}$/$RO^{\cdot}$ radicals produced by AAPH. Accordingly, our findings suggest that free radical scavenging by resveratrol leads to a wide range of valuable metabolites whose increased chemical complexity may also manifest in an unexpected increase in their overall antioxidant activity.

Supplementary Materials: The following are available online at www.mdpi.com/xxx/s1, Figures S1-S7: HPLC-PDA fingerprints of oxidized product mixtures Ox1-Ox7, Figures S8-S15: HRMS spectra of compounds **2**-**8**, Figures S16-S56: 1D and 2D NMR spectra of compounds **2**-**9**, Figures S57-S61: Lineweaver-Burk plots of compounds **2**-**6**.

Author Contributions: Conceptualization, A.H.; methodology, O.G.A., T.G., G.T., and A.H.; investigation, O.G.A., N.K., R.B., T.G., and G.T.; data curation, O.G.A., G.T. and A.H.; writing—original draft preparation, O.G.A., G.T., and A.H.; writing—review and editing, A.H.; supervision, A.H.; funding acquisition, A.H. All authors have read and agreed to the published version of the manuscript.

Funding: This work was supported by the National Research, Development and Innovation Office, Hungary (NKFIH; K-134704 and TKP2021-EGA-32 by the Ministry of Innovation and Technology of Hungary).

Data Availability Statement: Raw datasets are available from the authors upon request.

Conflicts of Interest: The authors declare no conflict of interest. The funders had no role in the design of the study; in the collection, analyses, or interpretation of data; in the writing of the manuscript, or in the decision to publish the results.

References

1. Dybkowska, E.; Sadowska, A.; Swiderski, F.; Rakowska, R.; Wysocka, K. The occurrence of resveratrol in foodstuffs and its potential for supporting cancer prevention and treatment. A review. *Rocz Panstw Zakl Hig* **2018**, *69*, 5-14.
2. Pannu, N.; Bhatnagar, A. Resveratrol: from enhanced biosynthesis and bioavailability to multitargeting chronic diseases. *Biomed Pharmacother* **2019**, *109*, 2237-2251, doi:10.1016/j.biopha.2018.11.075.
3. Baur, J.A.; Sinclair, D.A. Therapeutic potential of resveratrol: the in vivo evidence. *Nat Rev Drug Discov* **2006**, *5*, 493-506, doi:10.1038/nrd2060.

4. Jaklova Dytrtova, J.; Straka, M.; Belonoznikova, K.; Jakl, M.; Ryslava, H. Does resveratrol retain its antioxidative properties in wine? Redox behaviour of resveratrol in the presence of Cu(II) and tebuconazole. *Food Chem* **2018**, *262*, 221-225, doi:10.1016/j.foodchem.2018.04.096.
5. He, L.; He, T.; Farrar, S.; Ji, L.; Liu, T.; Ma, X. Antioxidants Maintain Cellular Redox Homeostasis by Elimination of Reactive Oxygen Species. *Cell Physiol Biochem* **2017**, *44*, 532-553, doi:10.1159/000485089.
6. Kelley, E.E.; Khoo, N.K.; Hundley, N.J.; Malik, U.Z.; Freeman, B.A.; Tarpey, M.M. Hydrogen peroxide is the major oxidant product of xanthine oxidase. *Free Radic Biol Med* **2010**, *48*, 493-498, doi:10.1016/j.freeradbiomed.2009.11.012.
7. Kumar, R.; Joshi, G.; Kler, H.; Kalra, S.; Kaur, M.; Arya, R. Toward an Understanding of Structural Insights of Xanthine and Aldehyde Oxidases: An Overview of their Inhibitors and Role in Various Diseases. *Med Res Rev* **2018**, *38*, 1073-1125, doi:10.1002/med.21457.
8. Tang, X.; Tang, P.; Ma, L.; Liu, L. Screening and Evaluation of Xanthine Oxidase Inhibitors from Gnetum parvifolium in China. *Molecules* **2019**, *24*, 2671, doi:10.3390/molecules24142671.
9. Jia, Z.; Zhu, H.; Misra, B.R.; Mahaney, J.E.; Li, Y.; Misra, H.P. EPR studies on the superoxide-scavenging capacity of the nutraceutical resveratrol. *Mol Cell Biochem* **2008**, *313*, 187-194, doi:10.1007/s11010-008-9756-y.
10. Walle, T. Bioavailability of resveratrol. *Ann N Y Acad Sci* **2011**, *1215*, 9-15, doi:10.1111/j.1749-6632.2010.05842.x.
11. Hunyadi, A. The mechanism(s) of action of antioxidants: From scavenging reactive oxygen/nitrogen species to redox signaling and the generation of bioactive secondary metabolites. *Med Res Rev* **2019**, *39*, 2505-2533, doi:10.1002/med.21592.
12. Springer, M.; Moco, S. Resveratrol and Its Human Metabolites-Effects on Metabolic Health and Obesity. *Nutrients* **2019**, *11*, 143, doi:10.3390/nu11010143.
13. Shingai, Y.; Fujimoto, A.; Nakamura, M.; Masuda, T. Structure and function of the oxidation products of polyphenols and identification of potent lipoxygenase inhibitors from Fe-catalyzed oxidation of resveratrol. *J Agric Food Chem* **2011**, *59*, 8180-8186, doi:10.1021/jf202561p.
14. Hunyadi, A.; Agbadua, O.G.; Takács, G.; Balogh, G.T. Scavengome of an Antioxidant. *ChemRxiv. Cambridge: Cambridge Open Engage* **2022**, preprint, doi:10.26434/chemrxiv-2022-jl7rs-v2.
15. Duddeck, H.; Dietrich, W.; Tóth, G. *Structure Elucidation by Modern NMR*; 1998; 10.1007/978-3-642-88310-1.
16. Pretsch, E.; Tóth, G.; Munk, E.M.; Badertscher, M. *Computer-Aided Structure Elucidation*; Wiley-VCH: 2002.
17. Duong, N.T.; Vinh, P.D.; Thuong, P.T.; Hoai, N.T.; Thanh, L.N.; Bach, T.T.; Nam, N.H.; Anh, N.H. Xanthine oxidase inhibitors from Archidendron clypearia (Jack.) I.C. Nielsen: Results from systematic screening of Vietnamese medicinal plants. *Asian Pac J Trop Med* **2017**, *10*, 549-556, doi:10.1016/j.apjtm.2017.06.002.
18. Fukumoto, L.R.; Mazza, G. Assessing antioxidant and prooxidant activities of phenolic compounds. *J Agric Food Chem* **2000**, *48*, 3597-3604, doi:10.1021/jf000220w.
19. Davalos, A.; Gomez-Cordoves, C.; Bartolome, B. Extending applicability of the oxygen radical absorbance capacity (ORAC-fluorescein) assay. *J Agric Food Chem* **2004**, *52*, 48-54, doi:10.1021/jf0305231.
20. Fasi, L.; Di Meo, F.; Kuo, C.Y.; Stojkovic Buric, S.; Martins, A.; Kusz, N.; Beni, Z.; Dekany, M.; Balogh, G.T.; Pesic, M., et al. Antioxidant-Inspired Drug Discovery: Antitumor Metabolite Is Formed in Situ from a Hydroxycinnamic Acid Derivative upon Free-Radical Scavenging. *J Med Chem* **2019**, *62*, 1657-1668, doi:10.1021/acs.jmedchem.8b01994.
21. Fasi, L.; Latif, A.D.; Zupko, I.; Levai, S.; Dekany, M.; Beni, Z.; Konczol, A.; Balogh, G.T.; Hunyadi, A. AAPH or Peroxynitrite-Induced Biorelevant Oxidation of Methyl Caffeate Yields a Potent Antitumor Metabolite. *Biomolecules* **2020**, *10*, 1537, doi:10.3390/biom10111537.
22. Forman, H.J.; Zhang, H.; Rinna, A. Glutathione: overview of its protective roles, measurement, and biosynthesis. *Mol Aspects Med* **2009**, *30*, 1-12, doi:10.1016/j.mam.2008.08.006.

23. Lee, D.; Bhat, K.P.; Fong, H.H.; Farnsworth, N.R.; Pezzuto, J.M.; Kinghorn, A.D. Aromatase inhibitors from Broussonetia papyrifera. *J Nat Prod* **2001**, *64*, 1286-1293, doi:10.1021/np010288l.
24. Li, X.Z.; Wei, X.; Zhang, C.J.; Jin, X.L.; Tang, J.J.; Fan, G.J.; Zhou, B. Hypohalous acid-mediated halogenation of resveratrol and its role in antioxidant and antimicrobial activities. *Food Chem* **2012**, *135*, 1239-1244, doi:10.1016/j.foodchem.2012.05.043.
25. Lee, H.J.; Seo, J.W.; Lee, B.H.; Chung, K.H.; Chi, D.Y. Syntheses and radical scavenging activities of resveratrol derivatives. *Bioorg Med Chem Lett* **2004**, *14*, 463-466, doi:10.1016/j.bmcl.2003.10.038.
26. D'Orsi, R.; Morrongiello, F.; Laurita, T.; Funicello, M.; Lupattelli, P.; Chiummiento, L. Regio- and Diastereo-Selective Biomimetic Synthesis of (±)-ϵ-Viniferin by NIS and Resveratrol. *ChemistrySelect* **2021**, *6*, 6863-6866, doi:10.1002/slct.202101678.
27. Ngoc, T.M.; Minh, P.T.; Hung, T.M.; Thuong, P.T.; Lee, I.; Min, B.S.; Bae, K. Lipoxygenase inhibitory constituents from rhubarb. *Arch Pharm Res* **2008**, *31*, 598-605, doi:10.1007/s12272-001-1199-0.
28. Pezet, R.; Perret, C.; Jean-Denis, J.B.; Tabacchi, R.; Gindro, K.; Viret, O. Delta-viniferin, a resveratrol dehydrodimer: one of the major stilbenes synthesized by stressed grapevine leaves. *J Agric Food Chem* **2003**, *51*, 5488-5492, doi:10.1021/jf030227o.
29. Yu, B.B.; Han, X.Z.; Lou, H.X. Oligomers of resveratrol and ferulic acid prepared by peroxidase-catalyzed oxidation and their protective effects on cardiac injury. *J Agric Food Chem* **2007**, *55*, 7753-7757, doi:10.1021/jf0711486.
30. Lindgren, A.E.G.; Öberg, C.T.; Hillgren, J.M.; Elofsson, M. Total Synthesis of the Resveratrol Oligomers (±)-Ampelopsin B and (±)-ϵ-Viniferin. *Eur J Org Chem* **2016**, *2016*, 426-429, doi:10.1002/ejoc.201501486.
31. Velu, S.S.; Di Meo, F.; Trouillas, P.; Sancho-Garcia, J.C.; Weber, J.F. Regio- and stereocontrolled synthesis of oligostilbenoids: theoretical highlights at the supramolecular level. *Journal of natural products* **2013**, *76*, 538-546, doi:10.1021/np300705p.
32. Bonechi, C.; Martini, S.; Magnani, A.; Rossi, C. Stacking interaction study of *trans*-resveratrol (*trans*-3,5,4'-trihydroxystilbene) in solution by Nuclear Magnetic Resonance and Fourier Transform Infrared Spectroscopy. *Magn Reson Chem* **2008**, *46*, 625-629, doi:10.1002/mrc.2217.
33. Naiker, M.; Anderson, S.; Johnson, J.B.; Mani, J.S.; Wakeling, L.; Bowry, V. Loss of trans-resveratrol during storage and ageing of red wines. *Aust J Grape Wine Res* **2020**, *26*, 385-387, doi:10.1111/ajgw.12449.
34. Hunyadi, A.; Martins, A.; Danko, B.; Chuang, D.-W.; Trouillas, P.; Chang, F.-R.; Wu, Y.-C.; Falkay, G. Discovery of the first non-planar flavonoid that can strongly inhibit xanthine oxidase: protoapigenone 1′ -*O*-propargyl ether. *Tetrahedron Lett* **2013**, *54*, 6529-6532, doi:10.1016/j.tetlet.2013.09.087.
35. Cao, H.; Pauff, J.M.; Hille, R. Substrate orientation and catalytic specificity in the action of xanthine oxidase: the sequential hydroxylation of hypoxanthine to uric acid. *J Biol Chem* **2010**, *285*, 28044-28053, doi:10.1074/jbc.M110.128561.
36. Ribeiro, P.M.G.; Fernandes, H.S.; Maia, L.B.; Sousa, S.F.; Moura, J.J.G.; Cerqueira, N.M.F.S.A. The complete catalytic mechanism of xanthine oxidase: a computational study. *Inorg Chem Front* **2021**, *8*, 405-416, doi:10.1039/d0qi01029d.
37. Nagao, A.; Seki, M.; Kobayashi, H. Inhibition of xanthine oxidase by flavonoids. *Biosci Biotechnol Biochem* **1999**, *63*, 1787-1790, doi:10.1271/bbb.63.1787.
38. Teles Fujishima, M.A.; Silva, N.; Ramos, R.D.S.; Batista Ferreira, E.F.; Santos, K.; Silva, C.; Silva, J.O.D.; Campos Rosa, J.M.; Santos, C. An Antioxidant Potential, Quantum-Chemical and Molecular Docking Study of the Major Chemical Constituents Present in the Leaves of Curatella americana Linn. *Pharmaceuticals* **2018**, *11*, 72, doi:10.3390/ph11030072.
39. Liu, L.; Zhang, L.; Ren, L.; Xie, Y. Advances in structures required of polyphenols for xanthine oxidase inhibition. *Food Front* **2020**, *1*, 152-167, doi:10.1002/fft2.27.
40. Liang, N.; Kitts, D.D. Antioxidant property of coffee components: assessment of methods that define mechanisms of action. *Molecules* **2014**, *19*, 19180-19208, doi:10.3390/molecules191119180.
41. Gülçin, İ. Antioxidant properties of resveratrol: A structure–activity insight. *Innov Food Sci Emerg Technol* **2010**, *11*, 210-218, doi:10.1016/j.ifset.2009.07.002.

42. Lin, J.; Li, X.; Chen, B.; Wei, G.; Chen, D. *E*-Configuration Improves Antioxidant and Cytoprotective Capacities of Resveratrols. *Molecules* **2018**, *23*, doi:10.3390/molecules23071790.
43. Intagliata, S.; Spadaro, A.; Lorenti, M.; Panico, A.; Siciliano, E.A.; Barbagallo, S.; Macaluso, B.; Kamble, S.H.; Modica, M.N.; Montenegro, L. In Vitro Antioxidant and Anti-Glycation Activity of Resveratrol and Its Novel Triester with Trolox. *Antioxidants* **2020**, *10*, 12, doi:10.3390/antiox10010012.
44. Lee, C.Y.; Nanah, C.N.; Held, R.A.; Clark, A.R.; Huynh, U.G.; Maraskine, M.C.; Uzarski, R.L.; McCracken, J.; Sharma, A. Effect of electron donating groups on polyphenol-based antioxidant dendrimers. *Biochimie* **2015**, *111*, 125-134, doi:10.1016/j.biochi.2015.02.001.
45. Lee, C.Y.; Sharma, A.; Semenya, J.; Anamoah, C.; Chapman, K.N.; Barone, V. Computational Study of Ortho-Substituent Effects on Antioxidant Activities of Phenolic Dendritic Antioxidants. *Antioxidants* **2020**, *9*, 189, doi:10.3390/antiox9030189.
46. Capaldo, L.; Ravelli, D. Hydrogen Atom Transfer (HAT): A Versatile Strategy for Substrate Activation in Photocatalyzed Organic Synthesis. *Eur J Org Chem* **2017**, *2017*, 2056-2071, doi:10.1002/ejoc.201601485.
47. Li, C.; Xu, X.; Tao, Z.; Wang, X.J.; Pan, Y. Resveratrol dimers, nutritional components in grape wine, are selective ROS scavengers and weak Nrf2 activators. *Food Chem* **2015**, *173*, 218-223, doi:10.1016/j.foodchem.2014.09.165.
48. Lopez-Alarcon, C.; Fuentes-Lemus, E.; Figueroa, J.D.; Dorta, E.; Schoneich, C.; Davies, M.J. Azocompounds as generators of defined radical species: Contributions and challenges for free radical research. *Free Radic Biol Med* **2020**, *160*, 78-91, doi:10.1016/j.freeradbiomed.2020.06.021.